Discretization and Solution of the Thermal Radiation Transport Equation in the Non-Relativistic Stellar Regime

Jim E. Morel

Texas A&M University
Department of Nuclear Engineering
College Station, TX 77843-3133
morel@tamu.edu

Overview

- The thermal radiation transport equation in static media

  - The equations of thermal radiation transport

  - The analytic equilibrium-diffusion limit

  - Asymptotic-preserving discretization

  - Angular, energy, spatial, and temporal discretization

  - Solution of the transport equation

    - Source Iteration

    - Diffusion-Synthetic Acceleration (DSA)

    - Linear Multifrequency Grey Acceleration (LMFGA)

    - Preconditioned Krylov adaptation of LMFGA

Overview

- Thermal radiation transport equation with non-relativistic material motion $(u/c < 0.01)$.

  - The physical effect of material motion on the lab-frame equations.

  - The comoving frame.

  - The relativistic lab-frame transport equation.

  - The $\mathrm{O}(u/c)$ lab-frame transport equation.

  - A simplified lab-frame transport equation for continuum transport.

- The nonrelativistic radiation-hydrodynamics equations

  - The nonrelativistic radiation-hydrodynamics equations in generic form.

  - Example solution algorithm for the radiation-hydrodynamics equations.

  - Future efforts.

Basic Equations

- The equations of thermal radiation transport consist of a transport equation for the angular intensity $I(\overrightarrow{r}, \overrightarrow{\Omega}, E, t)$:

$$\frac{1}{c}\frac{\partial I}{\partial t} + \overrightarrow{\Omega} \cdot \overrightarrow{\nabla} I + \sigma_t I = \frac{\sigma_s}{4\pi}\phi + \sigma_a B(T),$$

and an equation for the material temperature $T(\overrightarrow{r}, t)$:

$$C_v\frac{\partial T}{\partial t} = \int_0^\infty \sigma_a[\,\phi - 4\pi B(T)\,]\,dE.$$

Basic Equations

- The angular intensity has units of
  $(energy/area - time - steradian - energy),$

- $\overrightarrow{\Omega}$ is the photon direction vector,

- $E = h\nu \ (energy)$ is the photon energy,

- $c \ (length/time)$ is the speed of light,

- $\sigma_t(\overrightarrow{r}, E, T) \ (length^{-1})$ is the total macroscopic cross section,

- $\sigma_s(\overrightarrow{r}, T) \ (length^{-1})$ is the Thompson macroscopic scattering cross section,

- $\phi(\overrightarrow{r}, E, t) \ (energy/area - time - energy)$ is angle-integrated intensity,

- $C_v(\overrightarrow{r}, T) \ (energy/volume - temperature)$ is the material heat capacity,

Basic Equations

- $B(E,T)$ $(energy/area - time - steradian - energy)$ is the Planck function:

$$B(E,T) = \frac{2E^3}{h^3 c^2} \left[\exp\left(\frac{E}{kT}\right) - 1 \right]^{-1} \quad,$$

- h is *Planck's constant*,

- k is *Boltzmann's constant*

- There are two other basic equations associated with the transport equation: the radiation energy and momentum equations.

Basic Equations

- The radiation energy equation is obtained by integrating the transport equation over all directions and energies:

$$\frac{\partial \mathcal{E}}{\partial t} + \overrightarrow{\nabla} \cdot \overrightarrow{\mathcal{F}} = \int_0^\infty \sigma_a [\, 4\pi B(T) - \phi \,]\, dE \,.$$

where the radiation energy density $(energy/volume)$ is given by

$$\mathcal{E} \equiv \frac{1}{c} \int_0^\infty \int_{4\pi} I\left(\overrightarrow{\Omega}, E\right)\, d\Omega\, dE \,,$$

and the radiation flux $(energy - area - time)$ is given by

$$\overrightarrow{\mathcal{F}} \equiv \int_0^\infty \int_{4\pi} \overrightarrow{\Omega}\, I\left(\overrightarrow{\Omega}, E\right)\, d\Omega\, dE \,.$$

Basic Equations

- Note from the definition of $\mathcal{E}$ that the radiation intensity integrated over angle and energy $(energy - area - time)$, which we denote by φ, is equal to $c\mathcal{E}$.

- The radiation energy is an energy balance equation stating that the time rate of change of the radiation energy in a differential volume is equal to the energy sources minus the sinks.

- The radiation momentum equation is obtained by first multiplying the transport equation by $\overrightarrow{\Omega}/c$ and then integrating over all directions and energies:

$$\frac{1}{c^2}\frac{\partial \overrightarrow{\mathcal{F}}}{\partial t} + \overrightarrow{\nabla} \cdot \overrightarrow{\overrightarrow{\mathcal{P}}} + \int_0^\infty \frac{\sigma_a}{c}\overrightarrow{F}\,dE = 0\,,$$

Basic Equations

- where the radiation pressure $(energy/volume)$ is given by

$$\mathcal{P}_{i,j} \equiv \frac{1}{c} \int_0^\infty \int_{4\pi} \Omega_i \Omega_j I\left(\overrightarrow{\Omega}, E\right) \, d\Omega \, dE \,,$$

- The radiation momentum equation is a balance equation stating that the time rate of change of the radiation momentum in a differential volume is equal to the momentum sources minus the sinks.

- When we include material motion, the transport and hydrodynamics equations will be coupled.

- The radiation energy and momentum equations will be part of total (radiation plus material) energy and momentum conservation equations.

Nonlinearities

- Note that the radiative transfer equations have nonlinearities arising only from the temperature dependence of the material property coefficients and the Planck function.

- The heat capacity is generally a weak function of temperature, while the absorption cross sections are strong functions of temperature.

- The radiative transfer equations are generally solved using an approximate form of Newton's method.

- The method is approximate in that the non-linearities are usually not iterated to full consistency, and contributions to the Jacobian from the material property functions are neglected.

- Stability considerations require linearization of the Planck function but not the material property functions.

Connection with Neutronics

- The radiative transfer equations have much in common with the neutron transport equation.

- The regimes are quite different, but most of the computational technology developed for neutron transport has been applied over the last twenty years to the radiative transfer equation both in static media and with nonrelativistic material motion.

- Because radiative transfer calculations are much more demanding than neutron transport calculations, this connection has resulted in improvements in neutron transport methods that might not otherwise have occured.

- For the case of relativistic material motion, fundamentally new approaches may be required.

The Equilibrium-Diffusion Limit

- Under certain realizable physical conditions, the equations of radiative transfer reduce to a diffusion equation for the material temperature, with the radiation intensity given by the Planck function evaulated at the material temperature.

- This limit is known as equilibrium-diffusion limit. It is important because it often occurs in real systems, and it can be difficult for trnasport discretizations to accurately treat.

- The equilibrium-diffusion limit can be rigorously derived using an asymptotic expansion of the radiative transfer solution. The asymptotic expansion parameter is denoted by ϵ, and the diffusion limit is achieved as $\epsilon \to 0$.

The Equilibrium-Diffusion Limit

- The diffusion-limit equations are derived as follows.

  - Non-dimensionalize the equations of radiative transfer.

  - Identify appropriate non-dimensional physical parameters in these equations.

  - Scale each physical parameter by an appropriate power of ϵ.

  - Return the scaled equations to dimensional form.

  - Express the intensity and temperature solutions as power series in ϵ.

  - Substitute these series into the radiative transfer equations.

  - Expand all functions of the temperature in the radiative transfer equations in ϵ as well.

  - Create a heirarchical system of equations for the expansion coefficients of the intensity and temperature by successively equating all terms multiplied by each power of ϵ.

The Equilibrium-Diffusion Limit

- Manipulate these heirarchical equations to obtain the equations satisfied to leading-order by the intensity and temperature, i.e., the equilibrium diffusion limit equations.

- After nondimensionalization, the following nondimensional physical parameters arise:

  - $\frac{\lambda_{t,\infty}}{ct_\infty}$, the ratio of the characteristic time between photon interactions to the characteristic time scale of the intensity and temperature solutions.

  - $\frac{\lambda_\infty}{\ell_\infty}$, the ratio of the characteristic total photon mean-free-path to the characteristic length scale of the intensity and temperature solutions.

  - $\frac{\lambda_{t,\infty}}{\lambda_{s,\infty}}$, the ratio of the characteristic photon total mean-free-path to the characteristic photon scattering mean-free-path.

  - $\frac{C_v T_\infty c}{4\pi I_\infty E_\infty}$, the ratio of the material internal energy density to the radiation energy density.

The Equilibrium-Diffusion Limit

- The scaling is defined as follows:

    - $\dfrac{\lambda_{t,\infty}}{ct_\infty} \longrightarrow \epsilon^2.$

    - $\dfrac{\lambda_\infty}{\ell_\infty} \longrightarrow \epsilon.$

    - $\dfrac{\lambda_{t,\infty}}{\lambda_{s,\infty}} \longrightarrow \epsilon.$

    - The previous scaling implies that $\dfrac{\lambda_{a,\infty}}{\lambda_{t,\infty}} \longrightarrow 1 - \epsilon.$

    - $\dfrac{C_v T_\infty c}{4\pi I_\infty E_\infty} \longrightarrow \epsilon^0.$

The Equilibrium-Diffusion Limit

- To leading order, the material temperature satisfies the following equation:

$$\left(C_v + 4aT^3\right)\frac{\partial T}{\partial t} - \overrightarrow{\nabla}\cdot\frac{4aT^3}{3\langle\sigma_t\rangle}\overrightarrow{\nabla}T = 0\,,$$

where

$$\frac{1}{\langle\sigma_t\rangle} = \int_0^\infty \frac{1}{\sigma_t}\frac{\partial B}{\partial T}\,dE \bigg/ \int_0^\infty \frac{\partial B}{\partial T}\,dE\,.$$

- The intensity satisfies

$$I = B(E,T)\,.$$

Equilibrium-Diffusion Limit Boundary Layers

- If the intensity incident upon a diffusive region is non-Planckian, a boundary layer will be present in the intensity and temperature solutions within a few mean-free-paths of the boundary.

- The diffusion solution does not apply within the boundary layer.

- The effective boundary conditions for the diffusion solution on the interior depend upon the incident intensity.

- A boundary layer analysis must be applied to determine these conditions, and this unfortunately requires an exact solution of the radiative transfer equtions within the boundary layer.

- Accurate boundary conditions have been derived using approximate variational solutions.

Asymptotic Preserving Discretizations

- A discrete approximation to the radiative transfer equations is said to preserve the equilibrium diffusion limit if a valid discretization of the equilibrium diffusion limit equations is obtained when the asymptotic expansion is applied to the discrete equations.

- The term "valid discretization" simply implies a consistent or convergent discretization.

- However, it is desirable to have a robust discretization as well.

- Accurate (or at least physically-acceptable) interior diffusion solutions with unresolved boundary layers are also highly desirable since it can be very difficult to numerically resolve boundary layrers.

- Achieving asymptotic preservation is almost entirely a function of the spatial discretization scheme.

Asymptotic Preserving Discretizations

- For numerical purposes it is important to recognize that in the limit as $\epsilon \rightarrow 0$, the spatial scale length of the asymptotic solutions becomes infinite with respect to a mean-free-path.

- Thus in highly diffusive problems the spatial scalelength of the solution can be arbitrarily large with respect to the photon mean-free-path.

- An asymptotic-preserving discretization will yield accurate results in the diffusion limit as long as the spatial zoning resolves the variation of the asymptotic solution.

- A consistent but nonasymptotic-preserving discretization will only give accurate results if the cell widths are small with respect to a mean-free-path.

- This property can make it completely impractical to use nonasymptotic preserving schemes highly diffusive problems.

Angular Discretization

- We use the S_n or discrete-ordinates angular discretization, which is basically a collocation technique.

- The collocation points correspond to quadrature points on the unit sphere and the integration over angle is carried out using the quadrature formula.

- The discretized equations are:

$$\frac{1}{c}\frac{\partial I_m}{\partial t} + \overrightarrow{\Omega} \cdot \overrightarrow{\nabla} I_m + \sigma_t I_m = \frac{\sigma_s}{4\pi}\phi + \sigma_a B(T)\,, \quad m = 1, M,$$

and

$$C_v \frac{\partial T}{\partial t} = \int_0^\infty \sigma_a [\, \phi - 4\pi B(T) \,]\, dE\,.$$

where

$$I_m = I(\overrightarrow{\Omega}_m)\,, \quad \text{and} \quad \phi = \sum_{m=1}^M I_m w_m\,.$$

Angular Discretization

- The biggest weakness of the S_n method is non-physical "ray-effects" that arise in optically thin media with localized sources and are caused by a finite number of photon directions.

- The only other major discretization technique is the spherical-harmonic or P_n method.

- The P_n method can be viewed as a Galerkin method based upon a global spherical-harmonic trial space.

- The P_n method is rotationally invariant and thus has no ray effects, but it cannot treat rapid variations or discontinuities in the angular intensity.

- For instance, the P_n method badly smears shadows.

- Solution techniques are far more advanced for the S_n method.

Energy Discretization

- There is only one major energy discretization technique in use, and it is called the multigroup method.

- The multigroup method can be viewed as a Petrov-Galerkin method with a piecewise discontinuous trial space and a piecewise-constant weighting space.

- In particular, the energy domain is divided into G continuous intervals or groups, with the g'th group corresponding to $E \in \left(E_{g-\frac{1}{2}}, E_{g+\frac{1}{2}} \right)$

Energy Discretization

- The trial space representation for the intensity is

$$\tilde{I} = \sum_{g=1}^{G} I_g \beta_g(E) \,,$$

where the g'th basis function, β_g, is defined for all g to be zero for all energies not in group g and can have any desired dependence for energies within group g, subject to the following normalization:

$$\int_{E_{g-\frac{1}{2}}}^{E_{g+\frac{1}{2}}} \beta_g(E)\, dE = 1 \,.$$

Energy Discretization

- Integrating $\tilde{I}$ over group g, we find that I_g represents the integral of the angular intensity over group g:

$$I_g = \int_{E_{g-\frac{1}{2}}}^{E_{g+\frac{1}{2}}} \tilde{I}(E)\, dE \,.$$

- To ensure the correct equilibrium solution for the angular intensity, the Planck function must also be approximated in terms of the basis functions as follows:

$$\tilde{B} = \sum_{g=1}^{G} B_g \beta_g(E) \,,$$

where

$$B_g = \int_{E_{g-\frac{1}{2}}}^{E_{g+\frac{1}{2}}} B(E,T)\, dE \,.$$

Energy Discretization

- One generally defines the group basis function to have either a dependence corresponding to the Planck function, B, or to the temperature derivative of the Planck function, $\frac{\partial B}{\partial T}$, also known as the Rosselund function.

- The weight functions are defined for all g as follows:

$$
\begin{aligned}
W_g(E) &= 0 \quad \text{for all energies not in group } g, \\
&= 1 \quad \text{for all energies in group } g,
\end{aligned}
$$

- These weight functions ensure energy balance.

Energy Discretization

- The multigroup equations take the following form:

$$\frac{1}{c}\frac{\partial I_g}{\partial t} + \overrightarrow{\Omega} \cdot \overrightarrow{\nabla} I_g + \sigma_{t,g} I_g = \frac{\sigma_s}{4\pi}\phi_g + \sigma_{a,g} B_g(T), \quad g = 1, G,$$

and

$$C_v \frac{\partial T}{\partial t} = \sum_{g=1}^{G} \sigma_{a,g}[\, \phi_g - 4\pi B_g(T)\,]\, dE,$$

where

$$\phi_g = \int_{4\pi} I_g \, d\Omega,$$

Energy Discretization

- where

$$\phi_g = \int_{4\pi} I_g \, d\Omega \,,$$

and the multigroup cross sections represent averages over each group as follows:

$$\sigma_{a,g} = \int_{E_{g+\frac{1}{2}}}^{E_{g-\frac{1}{2}}} \sigma_a(E)\beta_g(E) \, dE \,,$$

$$\sigma_{s,g} = \int_{E_{g+\frac{1}{2}}}^{E_{g-\frac{1}{2}}} \sigma_s(E)\beta_g(E) \, dE \,,$$

with

$$\sigma_{t,g} = \sigma_{a,g} + \sigma_{s,g} \,.$$

Spatial Discretization

- The requirements for spatial discretization schemes are extremely demanding because:

  - Within a specific material region, the cross sections can vary with energy by many orders of magnitude.

  - The cross sections can change across a material interface by many orders of magnitude.

  - Problems often contain both optically-thin regions and optically-thick regions.

  - Optically thick regions may be strongly absorbing or highly diffusive.

  - In diffusive regions, the spatial scale-length of the solution can have a thickness of many mean-free paths (e.g., thousands or more).

Spatial Discretization

- It is not clear that one can afford to spatially resolve the transport solution in all regions even with an adaptive scheme.

- The desired characteristics of spatial discretization schemes are as follows:

  - Conservative.

  - Second-order accurate.

  - Asymptotic preserving.

  - Nearly positive and highly damped (robust).

- For the most part, finite-element discontinuous Galerkin (DG) methods have the first three properties, but lumping of both the gradient and interaction terms is generally required to achieve sufficient robustness.

- Let us initially consider the asymptotic properties of unlumped DG schemes.

Unlumped DG Properties

- The diffusion limit is never preserved with a constant DG trial-space.

- Linear or higher-order trial spaces preserve the diffusion limit on appropriate meshes.

- For instance, a linear DG trial space preserves the diffusion limit on triangles and tetrahedra, but a bilinear trial space must be used on quadrilaterals, and a trilinear trial space must be used on hexahedra.

- This effect is related to the fact that the discrete solution wants to become continuous in the diffusion limit, and if there are insufficient degrees of freedom in the trial space when this occurs, the scheme will be unable to accurately represent the solution and fail.
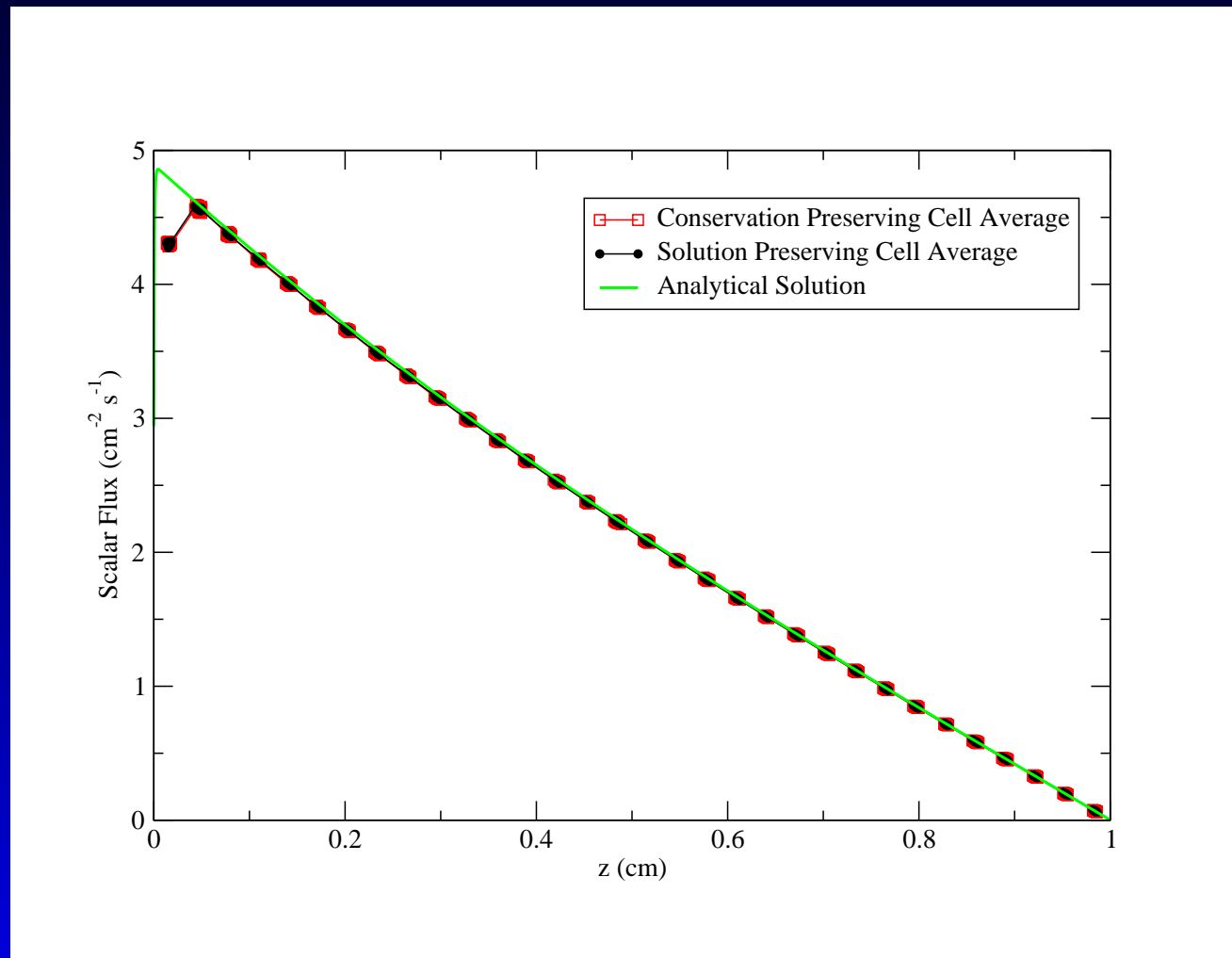
Unlumped DG Properties

- DG schemes can yield amazingly accurate interior solutions in the diffusion limit with unresolved spatial boundary layers.

- However, DG schemes do not yield the correct solution in the cell containing the unresolved boundary layer.
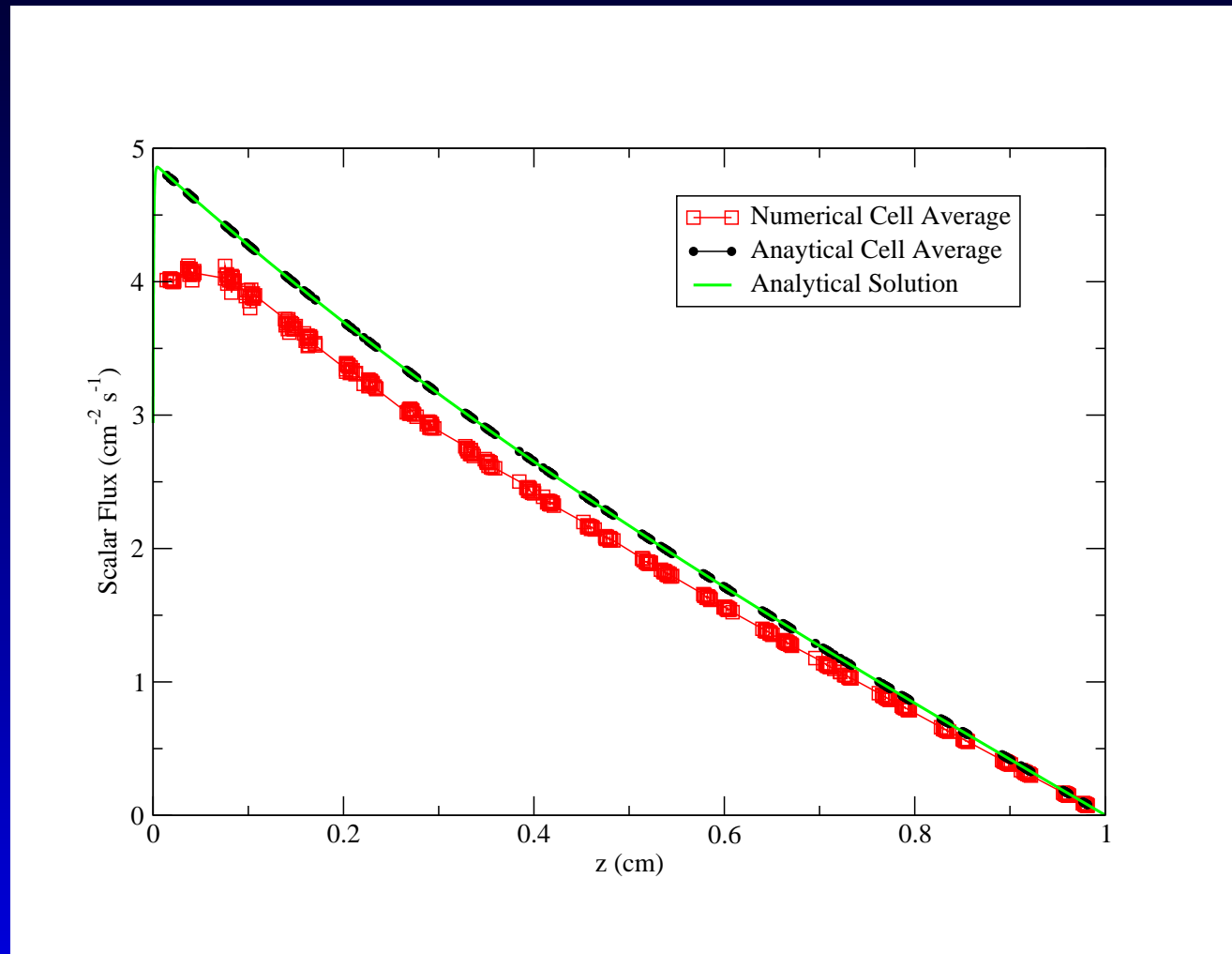
Unresolved Boundary Layer I

Quadrilateral-mesh DG solutions with an unresolved boundary layer.

Unresolved Boundary Layer II

Triangular-mesh DG solution with an unresolved boundary layer.

Lumped DG Schemes

- Finite-element lumping improves robustness by reducing the span of the stencil, but this also reduces accuracy.

- In the absence of superconvergence, the order accuracy can generally be maintained.

- Lumping of the interaction terms (standard mass-matrix lumping) is well understood and works well in essentially all cases, but lumping of the gradient terms remains a research topic.

- Considerable effort has been expended in recent years on lumping of linear-type DG discretizations on non-orthogonal finite-element meshes.

- Lumping is not difficult, but preserving the diffusion limit while lumping is difficult.

Lumped DG Schemes

- It has recently been found that non-orthogonal meshes significantly restrict gradient lumping.

- As a result we expect to see more research on higher-order DG discretizations since it is conceivable that lumping may not be necessary with such discretizations.

Lumped DG Schemes

- Let's consider a simple example problem to demonstrate discontinuous Galerkin methods and lumping:

$$\frac{\partial f}{\partial x} + \sigma f = 0 \,, \quad \text{for } x \in [0, h] \text{, with } f(0) = 1,$$

- The solution to this equation is $f(x) = \exp(-\sigma x)$.

- We will apply the linear discontinuous Galerkin method to this equation.

- The trial-space is defined as follows:

$$
\begin{aligned}
\tilde{f}(x) \;&=\; 1 \,, \quad \text{for } x = 0, \\
&=\; f_L \frac{h - x}{h} + f_R \frac{x}{h} \,, \quad \text{otherwise.}
\end{aligned}
$$

Lumped DG Schemes

- The equations for f_L and f_R are

$$\frac{1}{2}\left(f_R + f_L\right) - 1 + \left(\frac{2}{3}f_L + \frac{1}{3}f_R\right)h = 0\,,$$

  and

$$f_R - \frac{1}{2}\left(f_R + f_L\right) + \left(\frac{2}{3}f_R + \frac{1}{3}f_L\right)h = 0\,.$$

- Solving these equations for f_R, we obtain

$$f_R = \frac{1 - \frac{1}{3}\sigma h}{1 + \frac{1}{6}\sigma h + \sigma^2 h^2}\,.$$

- This is a superconvergent third-order accurate approximation to $\exp(-\sigma h)$, but the solution becomes negative for $\sigma h > 3$ eventually reaching a mimimum of of roughly -0.1.

Lumped DG Schemes

- Lumping the interaction terms, the equations for f_L and f_R become

$$\frac{1}{2}\left(f_R + f_L\right) - 1 + f_L h = 0\,,$$

and

$$f_R - \frac{1}{2}\left(f_R + f_L\right) + f_R h = 0\,.$$

- Solving these equations for f_R, we obtain

$$f_R = \frac{1}{1 + \sigma h + \frac{1}{2}\sigma^2 h^2}\,.$$

- This is a second-order accurate approximation to $\exp(-\sigma h)$ that is strictly positive.

Time discretization

- Surprisingly, little research has been traditionally been done on time-integration of the radiative transfer equations.

- The backward-Euler method is often applied. It is compatible with standard transport solution techniques, but it is only first-order accurate.

- The Crank-Nicholson method is second-order accurate, represents a minor variation on the backward-Euler method, and is similarly compatible with standard transport solution techniques. However, it is highly oscillatory.

- The linear discontinuous Galerkin method is second-order accurate and non-oscillatory, but it's use can significantly complicate the solution process.

Time discretization

- We are now investigating a variation of the "trapezoidal-BDF-2" method, that is second-order accurate, non-oscillatory, and compatible with standard transport solution techniques.

- For instance, let us consider a simple nonlinear equation of the following form:

$$\frac{\partial f}{\partial t} = \mathcal{A}f \, ,$$

where f is the solution and $\mathcal{A}$ is an operator that depends upon f, but is a linear operator for fixed f. This is analogous to the radiative transfer equations with the Planck function linearized.

Time discretization

- Then our scheme can be expressed in predictor-corrector form as follows, where n is the time index:

$$\frac{f^{n+\frac{1}{2}} - f^n}{\Delta t/2} = \mathbf{A}^n \left(\frac{f^{n+\frac{1}{2}} + f^n}{2} \right),$$

$$\frac{f^{n+1} - f^n}{\Delta t} = \mathbf{A}^{n+\frac{1}{2}} \left(\frac{f^{n+1} + f^{n+\frac{1}{2}} + f^n}{3} \right).$$

- In effect, two sequential solutions must be performed rather than one, but standard transport solution techniqes can be used for each one.

Time discretization

- For the case of a linear operator $\mathbf{A}$, this scheme is equivalent to performing one half-step using Crank-Nicholson followed by another half-step using the BDF-2 (Gear) formula:

$$\frac{f^{n+\frac{1}{2}} - f^n}{\Delta t/2} = \mathbf{A} \left(\frac{f^{n+\frac{1}{2}} + f^n}{2} \right) ,$$

$$\frac{\frac{3}{2}\left(f^{n+1} - f^{n+\frac{1}{2}}\right) - \frac{1}{2}\left(f^{n+\frac{1}{2}} - f^n\right)}{\Delta t/2} = \mathbf{A}\, f^{n+1} .$$

Solution of the Radiative Transfer Equations

- Traditional accelerated iterative solution techniques for the transport equation are closely related to multilevel or multigrid methods.

- In most instances, some type of diffusion operator is used to approximate a transport operator.

- For many years, such methods were thought to be unconditionally effective as long as the diffusion equations were differenced in a manner consistent with the spatial discretization of the transport operator.

- Unfortunately, when discontinuous Galerkin methods are used for the transport equation, the consistent diffusion discretizations are of a mixed form and can be very expensive to solve.

Solution of the Radiative Transfer Equations

- A great deal of research effort has been spent over the last 20 years or so to find ways to either use simpler diffusion discretizations or solve the full discretizations in an approximate manner without significant loss of effectiveness.

- These efforts have met with limited success.

- Furthermore, over the last five years or so, it has been recognized that traditional acceleration techniques are not uniformly effective in multidimensional calculations even when consistent diffusion discretizations are used.

- In particular, it has been found that strong material inhomogeneities can degrade effectiveness and occasionally generate instabilities.

Solution of the Radiative Transfer Equations

- It has now become clear that by recasting traditional accelerated iteration schemes as preconditioned Krylov methods, far greater lattitude in the choice of diffusion discretization is possible, the degrading effects of strong material inhomogeneities can be significantly reduced, and any associated instabilities eliminated.

- Consequently, there is currently a great deal of research within the computational transport community devoted to preconditioned Krylov methods.

Solution of the Radiative Transfer Equations

- As previously noted, the radiative transfer equations are generally solved via an approximate form of Newton's method.

- After linearization, temporal discretization (backward-Euler), and energy discretization (multigroup), we are able to eliminate the temperature from the transport equation:

$$
\overrightarrow{\Omega} \cdot \overrightarrow{\nabla} I_g + \sigma^*_{\tau,g} I = \frac{1}{4\pi} \sigma^*_{s,g} \phi_g + \frac{1}{4\pi} \nu \chi_g \sum_{k=1}^{G} \sigma^*_{a,k} \phi_k + \xi_g \ , \quad g = 1, G,
$$

- and an intensity-dependent temperature equation:

$$
T = T^* +
$$

$$
\frac{\sum_{g=1}^{G} \sigma^*_{a,g} \left[\phi_g - 4\pi B^*_g \right] + \frac{C^*_v}{\Delta t^k} \left(T^n - T^* \right)}{\frac{C^*_v}{\Delta t^k} + \sum_{g=1}^{G} \sigma^*_{a,g} 4\pi \frac{\partial B^*_g}{\partial T}} \ ,
$$

The Equations of Thermal Radiation Transport

- where

$$\sigma_\tau = \sigma_t + \tau\,,$$

$$\tau = \frac{1}{c\Delta t^k}\,,$$

$$\nu = \frac{\sum_{g=1}^{G}\sigma_{a,g}^* 4\pi \frac{\partial B_g^*}{\partial T}}{\frac{C_v^*}{\Delta t^k} + \sum_{g=1}^{G}\sigma_{a,g}^* 4\pi \frac{\partial B_g^*}{\partial T}}$$

$$\chi_g = \frac{\sigma_{a,g}^* \frac{\partial B_g^*}{\partial T}}{\sum_{k=1}^{G}\sigma_{a,k}^* \frac{\partial B_k^*}{\partial T}}\,,$$

$$\xi_g = \sigma_{a,g}^* B_g^* + \tau \psi_g^n -$$

$$\frac{1}{4\pi}\nu\chi_g \left[\sum_{k=1}^{G}\sigma_{a,k}^* 4\pi B_k^* + \frac{C_v^*}{\Delta t^k}\left(T^n - T^*\right)\right]\,.$$

Source Iteration

- The traditional method for solving the transport equation is a nested source iteration.

- Denoting the iteration index by ℓ, the inner iteration can be represented as follows:

$$\overrightarrow{\Omega} \cdot \overrightarrow{\nabla} I_g^{\ell+1} + \sigma_{\tau,g}^* I_g^{\ell+1} = \frac{1}{4\pi}\sigma_{s,g}^* \phi_g^\ell + \frac{1}{4\pi}\nu\chi_g \sum_{k=1}^{G} \sigma_{a,k}^* \phi_k + \xi_g\,,$$

- and the outer iteration can be represented as follows:

$$\overrightarrow{\Omega} \cdot \overrightarrow{\nabla} I_g^{\ell+1} + \sigma_{\tau,g}^* I_g^{\ell+1} - \frac{1}{4\pi}\sigma_{s,g}^* \phi_g^{\ell+1} = \frac{1}{4\pi}\nu\chi_g \sum_{k=1}^{G} \sigma_{a,k}^* \phi_k^\ell + \xi_g\,.$$

Source Iteration

- The operator $\overrightarrow{\Omega} \cdot \overrightarrow{\nabla} + \sigma^*_{\tau,g}$ involves no angular or energy coupling.

- When spatially discretized it takes on a block lower-triangular form with a block corresponding to the intensities within a single spatial cell for a single direction and energy.

- This operator is easily inverted using a "wavefront" or "sweep" algorithm.

- The attenuation of errors in ϕ_g determines the convergence rate of the inner iteration process.

- The attenuation of errors in $f = \sum_{g=1}^{G} \sigma^*_{a,g} \phi_g$ determines the convergence rate of the outer iteration process.

Source Iteration

- The inner iteration process can become arbitrarily slow to converge as $\sigma^*_{s,g} \rightarrow \sigma^*_{\tau,g}$. This corresponds to scattering dominating absorption.

- The outer iteration can become arbitrarily slow to converge as $\nu \rightarrow 1$ and $\tau \rightarrow 0$. This physically corresponds to strong material-radiation coupling (small heat capacity and large absorption cross section).

- For the case of an infinite homogeneous medium, Fourier analysis can be used to demonstrate that the most slowly converging error modes for both iterations are those that slowly vary in space.

- Thus the inversion of the advection-reaction operator is a form of relaxation: high-frequency errors are strongly attenuated, while low-frequency errors are poorly attenuated.

Diffusion-Synthetic Acceleration

- Inner source iteration with diffusion-synthetic acceleration (DSA) takes the following form:

$$\overrightarrow{\Omega} \cdot \overrightarrow{\nabla} I_g^{\ell+\frac{1}{2}} + \sigma_{\tau,g}^* I_g^{\ell+\frac{1}{2}} = \frac{1}{4\pi} \sigma_{s,g}^* \phi_g^\ell + \frac{1}{4\pi} \nu \chi_g \sum_{k=1}^{G} \sigma_{a,k}^* \phi_k + \xi_g \,,$$

$$-\overrightarrow{\nabla} \cdot \frac{1}{3\sigma_{\tau,g}^*} \overrightarrow{\nabla} \delta\phi_g + \left(\sigma_{\tau,g}^* - \sigma_{s,g}^* \right) \delta\phi_g = \sigma_{s,g}^* \left(\phi_g^{\ell+\frac{1}{2}} - \phi_g^\ell \right) \,,$$

$$\phi_g^{\ell+1} = \phi_g^{\ell+\frac{1}{2}} + \delta\phi_g \,.$$

Diffusion-Synthetic Acceleration

- For the case of an infinite homogeneous medium, Fourier analysis can be used to demonstrate that this scheme completely attenuates the low-frequency error modes and grossly underestimates the high-frequency error modes.

- This is the best one can hope for in an approximate inverse.

- The scheme is unconditionally effective in 1-D and only becomes ineffective in strongly heterogeneous multidimensional problems.

Linear Multifrequency-Grey Acceleration

- Outer source iteration with LMFGA takes the following form:

$$\overrightarrow{\Omega} \cdot \overrightarrow{\nabla} I_g^{\ell+\frac{1}{2}} + \sigma_{\tau,g}^* I_g^{\ell+\frac{1}{2}} - \frac{1}{4\pi} \sigma_{s,g}^* \phi_g^{\ell+\frac{1}{2}} = \frac{1}{4\pi} \nu \chi_g f^\ell + \xi_g \,,$$

$$-\overrightarrow{\nabla} \cdot \langle D \rangle \overrightarrow{\nabla} \delta\Phi + \left[\langle \sigma_a \rangle \left(1 - \nu \right) + \tau \right] \delta\Phi = f^{\ell+\frac{1}{2}} - f^\ell \,, \qquad (1)$$

$$f^{\ell+1} = f^{\ell+\frac{1}{2}} + \langle \sigma_a \rangle \delta\Phi \,,$$

Linear Multifrequency-Grey Acceleration

- where

$$\langle D \rangle = \sum_{g=1}^{G} \frac{\varsigma_g}{3\sigma_{\tau,g}^*} \, ,$$

$$\langle \sigma_a \rangle = \sum_{g=1}^{G} \sigma_{a,g}^* \varsigma_g \, ,$$

$$\varsigma_g = \frac{\dfrac{\chi_g}{\sigma_{\tau,g}^*}}{\sum_{k=1}^{G} \dfrac{\chi_k}{\sigma_{\tau,k}^*}} \, .$$

Linear Multifrequency-Grey Acceleration

- For the case of an infinite homogeneous medium, Fourier analysis can be used to demonstrate that this scheme completely attenuates the low-frequency error modes and grossly underestimates the high-frequency error modes.

- This is the best one can hope for in an approximate inverse.

- The scheme appears to be unconditionally effective in 1-D but can apparently become unstable in strongly heterogeneous multidimensional problems.

- This motivates us to develop a preconditioned Krylov method based upon the multifrequency-grey acceleration technique.

- Before deriving this scheme, we briefly discuss Krylov methods.

Krylov Methods

- The details of Krylov methods are not of importance for this discussion, but some knowledge is required.

- Suppose one wants to solve a linear system of the following basic form:

$$\mathbf{A}\,\vec{x} = \vec{y}\,,$$

where $\mathbf{A}$ is a matrix, $\vec{x}$ is the soultion vector, and $\vec{y}$ is the source vector.

- A Krylov method will construct an approximate solution to this equation from the space of Krylov vectors of dimension d:

$$\mathcal{K}_d = \left[r, \mathbf{A}\,\vec{r}, \mathbf{A}^2\,\vec{r}, \ldots, \mathbf{A}^{d-1}\,\vec{r} \right]\,,$$

where $\vec{r}$ is the residual associated with the initial guess, $\vec{x}_0$:

$$\vec{r} = \vec{y} - \mathbf{A}\,\vec{x}_0\,.$$

Krylov Methods

- There are many different types of Krylov solvers that construct this approximation in various ways.

-

- With most Krylov methods, the iteration process begins with an approximate solution constructed from $\mathcal{K}_1$ and proceeds to provide an approximate solution constructed from $\mathcal{K}_d$ on the d'th iteration.

- To use a Krylov solver, one must be able to evaluate the *action* of $\mathbf{A}$ on an arbitrary vector, $\overrightarrow{z}$, i.e., given $\overrightarrow{z}$, one must compute

$$\overrightarrow{v} = \mathbf{A}\,\overrightarrow{z}\,.$$

- It is important to recognize that one need not actually form the matrix $\mathbf{A}$ to evalutate its action.

Krylov Methods

- In many instances, the matrix $\mathbf{A}$ is dense and the action of $\mathbf{A}$ must be calculated in an indirect manner.

- This is the case for the matrix associated with our transport solution technique.

- Characterizing the convergence of Krylov methods for general matrices remains an open problem.

- However, there is one simple rule that can be followed: convergence will improve as the domain of the eigenvalues becomes smaller and as the domain moves away from the origin.

- Preconditioning can be used to improve convergence.

- We generally use only left preconditioning.

A Nested Preconditioned Krylov Method

- Left preconditioning is carried out simply by multiplying the original equation by another matrix:

$$\mathbf{PA}\,\vec{x} = \mathbf{P}\,\vec{y}\,,$$

  where the matrix $\mathbf{P}$ is called the preconditioner.

- Ideally, $\mathbf{P}$ would be the inverse of $\mathbf{A}$, but of course one would not be using a Krylov method if it were possible to form the action of $\mathbf{A}^{-1}$.

- An ideal practical choice for $\mathbf{P}$ is to make it approximate $\mathbf{A}^{-1}$ for the eigenvectors with eigenvalues closest to zero, and act as the identity for the remaining eigenvalues.

A Nested Preconditioned Krylov Method

- Our aim is to derive an equation for the absorption rate, f, from the equation for the intensity, I.

- The Krylov method will be used to solve a preconditioned variant of the equation for f.

- Once f is obtained, I can be obtained by solving G independent monoenergetic transport equations.

- We begin by expressing the transport equation in operator form:

$$\mathbf{A}_g I_g = \left[\frac{1}{4\pi} \nu \chi_g f + \xi_g \right] , \quad g = 1, G.$$

$$\mathbf{A}_g \equiv \overrightarrow{\Omega} \cdot \overrightarrow{\nabla} + \sigma^*_{\tau,g} - \frac{1}{4\pi} \sigma_{s,g} \mathbf{P} ,$$

$$\mathbf{P} \langle \cdot \rangle = \int_{4\pi} \langle \cdot \rangle \, d\Omega ,$$

A Nested Preconditioned Krylov Method

- Solving the transport equation for I_g, we obtain

$$I_g = \mathbf{A}_g^{-1} \left[\frac{1}{4\pi} \nu \chi_g f + \mathbf{A}_g^{-1} \xi_g \right] , \quad g = 1, G.$$

- Given f, this equation is solved via a preconditioned Krylov method to obtain I_g.

- Integrating the above equation over all directions, multiplying on the left by $\sigma_{\tau,g}^*$, and summing over all groups yields the desired equation for f:

$$\mathbf{B}f = \sum_{g=1}^{G} \sigma_{a,g}^* \mathbf{P} \mathbf{A}_g^{-1} \xi_g \, ,$$

$$\mathbf{B} = \left[\mathbf{I} - \sum_{g=1}^{G} \sigma_{a,g}^* \mathbf{P} \mathbf{A}_g^{-1} \frac{1}{4\pi} \nu \chi_g \right] ,$$

A Nested Preconditioned Krylov Method

- The action of $\mathbf{B}$ requires the solution of G independent monoenergetic transport equations.

- These equations must be solved via a preconditioned Krylov method, yielding an overall Krylov method that is nested.

- There are two advantages to solving the equation for f:

  - The rank of the f-equation is far less than that of the original transport equation - number of space points versus number of space points times number of energies times number of directions.

  - The transport operator is unbounded but $\mathbf{B}$ is compact with real eigenvalues between 0 and 1.

A Nested Preconditioned Krylov Method

- We left precondition the f equation with the operator $\mathbf{C}$:

$$\mathbf{CB}f = \mathbf{C}\sum_{g=1}^{G}\sigma_{a,g}^{*}\mathbf{PA}_{g}^{-1}\xi_{g}\,,$$

$$\mathbf{C} \equiv \left(\mathbf{I} + \langle\sigma_a\rangle\mathbf{H}^{-1}\nu\right)\,,$$

$$\mathbf{H} \equiv -\overrightarrow{\nabla}\cdot\langle D\rangle\overrightarrow{\nabla} + \left[\langle\sigma_a\rangle(1-\nu)+\tau\right]\,.$$

- Note that $\mathbf{H}$ is the diffusion operator from the LMFGA method.

- $\mathbf{C}$ is a very effective preconditioner.

- An infinite-medium Fourier analysis shows that $\mathbf{C}$ becomes the exact inverse of $\mathbf{B}$ when operating on eigenfunctions of $\mathbf{B}$ in the limit as the eigenvalue approaches zero.

A Nested Preconditioned Krylov Method

- There is a simple relationship between our preconditioned Krylov method and the linear multifrequency-grey acceleration technique.

- In particular, the accelerated iteration for the absorption rate can be expressed as follows:

$$f^{\ell+1} = f^{\ell} + \mathbf{C} \sum_{g=1}^{G} \sigma_{a,g}^{*} \mathbf{P} \mathbf{A}_g^{-1} \xi_g - \mathbf{C}\mathbf{B} f^{\ell},$$

- Note that this is just Richardson iteration on the system solved in our Krylov method.

A Nested Preconditioned Krylov Method

- We use a similar strategy for solving the group equations.

- We derive an equation for ϕ_g that has a lower rank than the original monoenergetic transport equation.

- The operator associated with this reduced-rank equation is compact with real eigenvalues between 0 and 1.

- We use a Krylov method to solve a preconditioned variant of this equation.

- The preconditioner contains the inverse of the diffusion operator associated with the DSA method, and is very effective because it moves the eigenvalues nearest zero to essentially one.

- Once ϕ_g has been obtained, I_g can be obtained via a solution of the block lower triangular advection-reaction equation.

A Nested Preconditioned Krylov Method

- The dominant effort required to apply the action of the overall preconditioned operator for f consists of:

  - A solution of a block lower-triangular equation and a DSA diffusion equation for each energy group and each inner preconditioned Krylov iteration.

  - A solution of the LMFGA diffusion equation.

- The diffusion equations themselves are solved via a precondioned Krylov method.

- If the diffusion solution technique is efficient, the transport solution technique will be efficient.

A Nested Preconditioned Krylov Method

- Our nested preconditioned transport method has not yet been tested, but a multigroup diffusion variant of it has been tested, and we will present some results here.

- The strategy of obtaining a reduced-rank equation cannot be applied unless the interaction operators are low-rank.

- If the interaction operators are full rank, effective preconditioners may or may not be constructed from from low-rank or coarse-grid approximate inverses.

- In some cases, full-rank interaction terms require true multigrid preconditioners.

- It may not always be optimal to use a reduced-rank equation.

- To illustrate this point, we consider a variant of our solution technique with the following properties: properties.

A Nested Preconditioned Krylov Method

- To illustrate this point, we consider a variant of our solution technique with the following properties:

  - The vector of angle-integrated intensities is the unknown rather than the vector of absorption rates.

  - The block lower-triangular advection-reaction equation is solved for each group rather than a transport equation for each group. Thus the cost per iteration will be lower.

  - Preconditioning is performed by solving a diffusion equation for each group and then by solving a grey diffusion equation.

A Nested Preconditioned Krylov Method

- It is not clear if the preconditioners will be as effective for this formulation as they are for absorption rate formulation.

- Thus it is unclear if the overall cost of this formulation will be reduced or increased relative to that of the absorption rate formulation.

- These methods can be formulated in many different ways.

- This field of research is largely unexplored and very rich.

A Multigroup Diffusion Example

- We have tested a method that solves the following equation:

$$-\overrightarrow{\nabla} \cdot D_g^* \overrightarrow{\nabla} \phi_g + \sigma_{\tau,g}^* \phi_g - \nu \chi_g \sum_{k=1}^{G} \sigma_{a,k}^* \phi_k = \xi_g\,, \quad g = 1, G,$$

- The method is analogous to our transport method.

- The only significant difference is that

$$\mathbf{A}_g \equiv -\overrightarrow{\nabla} \cdot D_g \overrightarrow{\nabla} + \sigma_{\tau,g}^*\,.$$

- Thus we solve a diffusion equation rather than a transport equation for each group.

A Multigroup Diffusion Example

- There are really only two material regions, the middle region facilitates non-uniform zoning.

- There are two problems: one with a uniform density everywhere and the other with a density jump of 1000 between the inner and outer regions - both were performed with the same 10-group cross sections.

- The radiation source is turned on at $t = 0$ and radiation propagates through the system.

Cylindrical Geometry for Diffusion Test Problems.
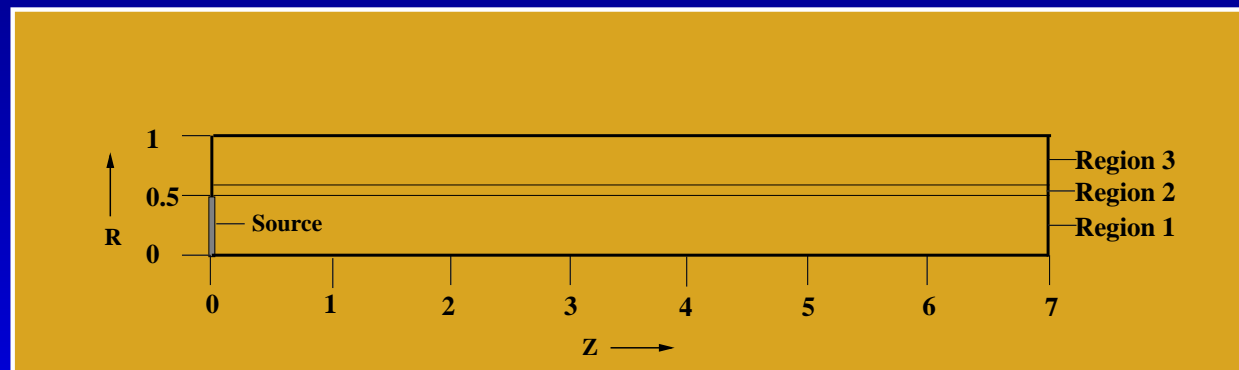
A Multigroup Diffusion Example

Comparisons for the variable–density calculations.

$\Delta t\,(sh)$	Method	Time (s)	No. of "Outer" Iterations	No. of "Inner" Iterations
0.1	LMFGK	327.2	7.98	1424.42
	LMFGA	679.1	25.73	2929.14
0.01	LMFGK	1776.7	3.55	668.40
	LMFGA	2353.6	8.07	785.00
0.001	LMFGK	9412.8	1.26	260.32
	LMFGA	11020.7	1.56	190.12

A Multigroup Diffusion Example

Comparisons for the uniform–density calculations.

$\Delta t\,(sh)$	Method	Time (s)	No. of "Outer" Iterations	No. of "inner" Iterations
0.2	LMFGK	62.8	3.41	455.71
	LMFGA	79.3	6.14	472.31
0.1	LMFGK	117.3	2.83	403.83
	LMFGA	139.4	4.57	376.99
0.01	LMFGK	897.7	1.228	249.49
	LMFGA	1014.4	1.375	180.97

A Multigroup Diffusion Example

Outer iteration counts as a function of time-step number for the variable–density problem with a 0.1 sh time step.
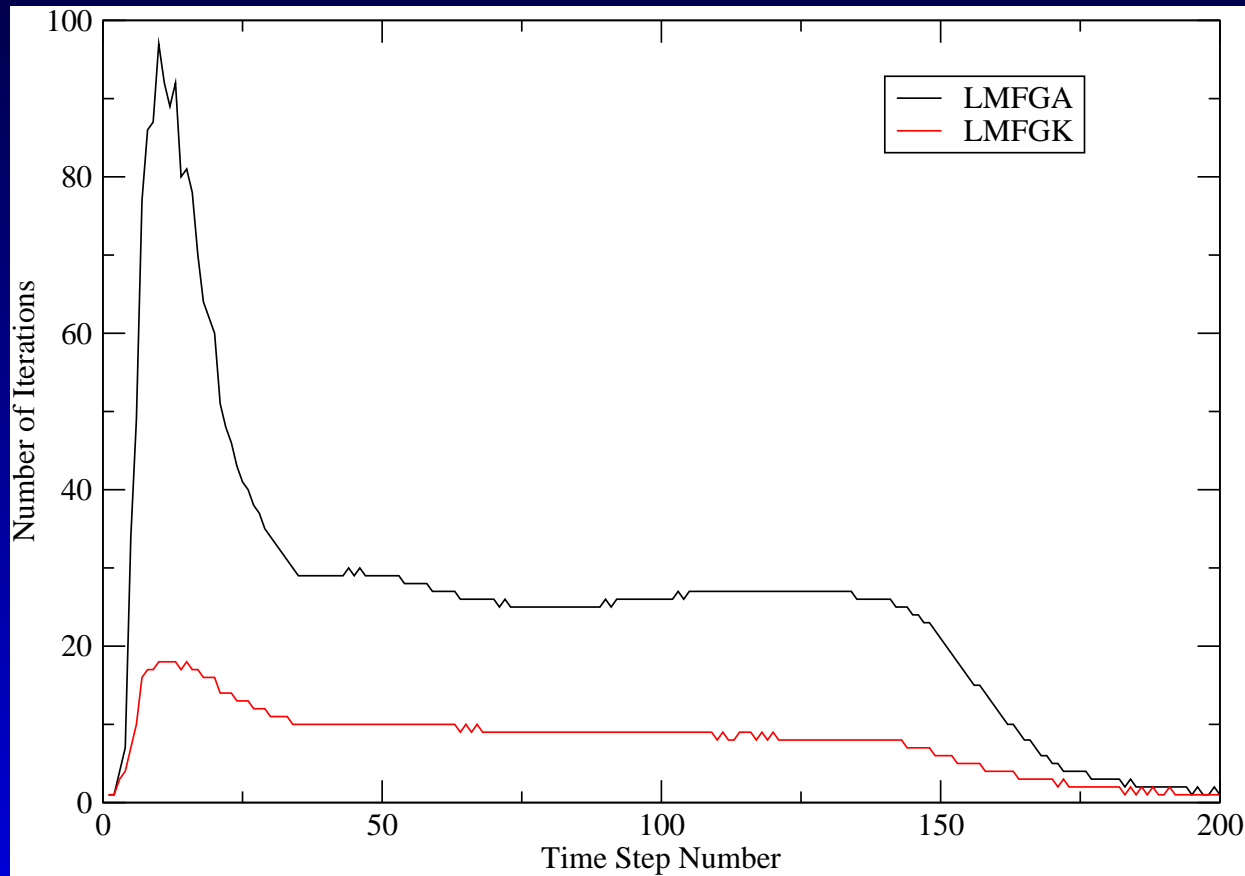
A Multigroup Diffusion Example

- The Krylov method always takes fewer iterations than the acceleration method.

- The Krylov method performs takes significantly few iterations with a large discontinuity in density.

- The relative CPU times are not proportional to the number of iterations because the Krylov method requires more time per outer iteration because more inner iterations are required with the Krylov method.

- This is an unexpected effect that is easily understood.

- The inner solves for the acceleration technique have increasingly better initial guesses as the solution converges - the guesses are the solutions from the previous outer iteration.

- The inner iteration solutions for the Krylov method are independent for each outer iteration, so an initial guess of zero is always used.

A Multigroup Diffusion Example

- The ratio of iterations between the two methods varies significantly between time steps.

- The acceleration method has been observed to go unstable in complex and highly heterogeneous calculations.

- The Krylov method has so far remained effective in such calculations.

- Heuristic methods have been developed to deal with the instabilities of the acceleration technique, but a robust method is always preferable.

The Physical Effect of Material Motion

- The radiative transfer equations for a static medium account for both radiation energy and radiation momentum deposition in the material, but they assume that the material motion induced by this deposition is negligible.

- When it is not, the fluid dynamics equations and the radiation transport equation must be coupled, yielding the radiation-hydrodynamics equations.

- We will defer a discussion of the radiation-hydrodynamics equations until we discuss the effect of material motion on the transport equation itself.

The Physical Effect of Material Motion

- In the lab frame, material motion simply has the effect of modifying the cross sections, which are defined in the rest frame of the material.

- It might be assumed that material motion can be neglected for continuum transport if the material speed is less than a percent of the speed of light, but care must be taken.

- Although the material motion correction terms are relatively small, neglecting them means that the change in the kinetic energy of the material due to momentum deposition by the photons will not be removed from the photon energy field.

- This imbalance can be significant over the course of an entire calculation even with very small material speeds.

The Comoving Frame

- In principle, one can treat material motion by recomputing the cross sections kinematically in the lab frame with material motion, but this would be onerous.

- An alternative is to apply an instantanous Lorentz transformation at each point and time to a frame that is locally at rest with respect to the material.

- This is called the comoving frame.

- The comoving-frame intensity, $I(t, \overrightarrow{r}, \overrightarrow{\Omega}_0, E_0)$, represent the intensity at lab-frame time t and lab-frame space point $\overrightarrow{r}$, seen in a frame moving at the local material velocity, $\overrightarrow{v}(t, \overrightarrow{r})$, due to photons with comoving direction $\overrightarrow{\Omega}_0$ and comoving energy E_0.

The Comoving Frame

- Comoving interaction rates are easily computed since the cross sections are valid in the comoving frame.

- Lorentz transformations together with physical principles, e.g., the number of photon interactions observed over a differential time must be identical in both frames, can be used to relate the lab-frame and comoving-frame interaction terms, thus making it possible to obtain the lab-frame equation in terms of the comoving frame cross sections.

- This equation is sometimes called the "mixed-frame" equation, but it is really just the lab-frame equation.

The Relativistic Lab-Frame Equation

- The relativistic lab-frame equation can be expressed as follows:

$$\frac{1}{c}\frac{\partial I}{\partial t} + \overrightarrow{\Omega}\cdot\overrightarrow{\nabla}I + (E_0/E)\sigma_t(E_0)I(\overrightarrow{\Omega},E) =$$

$$(E/E_0)^2\frac{\sigma_s}{4\pi}\int_{4\pi}(E_0/E')\,I(\overrightarrow{\Omega}',E')\,d\Omega' + (E/E_0)^2\,\sigma_a(E_0)B(E_0)\,,$$

where

$$E_0 = E\,\gamma\left(1 - \overrightarrow{\Omega}\cdot\overrightarrow{u}/c\right)\,,$$

$$\gamma = \left(1 - u^2/c^2\right)^{-\frac{1}{2}}\,,$$

$$E' = E\,\frac{1 - \overrightarrow{\Omega}\cdot\overrightarrow{u}/c}{1 - \overrightarrow{\Omega}'\cdot\overrightarrow{u}/c}\,.$$

The O(u/c) Lab-Frame Equation

- The relativistic lab-frame equation is sometimes expanded to O(u/c) for nonrelativistic applications:

$$\frac{1}{c}\frac{\partial I}{\partial t} + \overrightarrow{\Omega} \cdot \overrightarrow{\nabla} I + \sigma_t I = \frac{\sigma_s}{4\pi}\varphi + \sigma_a B +$$

$$\left[\left(\sigma_t + E\frac{\partial \sigma_a}{\partial E}\right) I + \frac{\sigma_s}{4\pi}\left(2\varphi - E\frac{\partial \varphi}{\partial E}\right) + 2\sigma_a B - B\,E\frac{\partial \sigma_a}{\partial E} - \sigma_a\,E\frac{\partial B}{\partial E}\right.$$

$$\frac{\sigma_s}{4\pi}\left(\overrightarrow{F} - E\frac{\partial \overrightarrow{F}}{\partial E}\right) \cdot \overrightarrow{u}\,/c\,.$$

A Simplified Lab-Frame Transport Equation

- Our primary intent is to accurately compute the exchange of energy and momentum between the radiation and material fields.

- Detailed radiation spectra are not of interest.

- We have derived an approximate lab-frame transport equation in accordance with these constraints that has the following properties when coupled with the hydrodynamic equations:

  - Total (radiation plus material) energy and momentum are conserved.

  - The correct equilibrium solutions for radiation energy density, radiation flux, and radiation pressure are obtained to $\mathrm{O}(u/c)$

  - The equilibrium-diffusion limit for radiation-hydrodynamics is preserved to $\mathrm{O}(u/c)$.

- The approximate equation is almost correct to $\mathrm{O}(u/c)$ in an integral sense with grey (frequency-independent) cross sections.

A Simplified Lab-Frame Transport Equation

- The simplified equation takes the form of the transport equation in a static medium plus a P_1-like correction term:

$$\frac{1}{c}\frac{\partial I_g}{\partial(}t) + \overrightarrow{\Omega} \cdot \overrightarrow{\nabla} I_g + \sigma_{t,g}I_g = \frac{\sigma_{s,g}}{4\pi}\phi_g + \sigma_{a,g}B_g +$$

$$\frac{1}{4\pi}C_{0,g} + \frac{3}{4\pi}\overrightarrow{C}_{1,g} \cdot \overrightarrow{\Omega},$$

where

$$C_{0,g} = -\sigma_{t,g}\left(\overrightarrow{F}_g - \frac{4}{3}\phi_g\frac{\overrightarrow{u}}{c}\right) \cdot \frac{\overrightarrow{u}}{c},$$

$$\overrightarrow{C}_{1,g} = \sigma_{t,g}\frac{4}{3}\phi_g\overrightarrow{u}.$$

A Simplified Lab-Frame Transport Equation

- The corresponding radiation energy and radiation momentum equations are respectively:

$$\frac{\partial \mathcal{E}}{\partial t} + \overrightarrow{\nabla} \cdot \overrightarrow{\mathcal{F}} = \sum_{g=1}^{G} \sigma_{a,g}[\, 4\pi B_g - \phi_g \,] - \sum_{g=1}^{G} \sigma_{a,g} \left(\overrightarrow{F}_g - \frac{4}{3}\phi_g \frac{\overrightarrow{u}}{c} \right) \cdot \frac{\overrightarrow{u}}{c} \,,$$

and

$$\frac{1}{c^2} \frac{\partial \overrightarrow{\mathcal{F}}_g}{\partial t} + \overrightarrow{\nabla} \cdot \overrightarrow{\overrightarrow{\mathcal{P}}}_g + \sum_{g=1}^{G} \frac{\sigma_{a,g}}{c} \overrightarrow{F}_g = \sum_{g=1}^{G} \frac{\sigma_{a,g}}{c} \frac{4}{3}\phi_g \frac{\overrightarrow{u}}{c} \,,$$

- The C_0 terms subtract the change in the material kinetic energy due to radiation momentum deposition from the radiation field.

A Simplified Lab-Frame Transport Equation

- The $\overrightarrow{C}_1$ terms ensure that the comoving-frame flux in equilibrium is given by

$$\overrightarrow{\mathcal{F}}_0 = \overrightarrow{\mathcal{F}} - \frac{4}{3}\mathcal{E}\,\overrightarrow{u}\,,$$

  which is correct through $\mathrm{O}(u/c)$, and they also ensure that there is no momentum deposition in equilibrium.

- Our approximation differentiates between the comoving-frame and lab-frame radiation fluxes, but effectively neglects the difference between the comoving-frame and lab-frame radiation energy densities.

- The maximum relative difference between E_0 and E is roughly 2 percent, but the relative difference between $\overrightarrow{\mathcal{F}}_0$ and $\overrightarrow{\mathcal{F}}$ is infinite.

- While $\overrightarrow{\mathcal{F}}$ has a magnitude in equilibrium of roughly 1 percent of $c\mathcal{E}$, $\overrightarrow{\mathcal{F}}_0$ in equilibrium is zero.